Gene Expression, Vol. 12, pp. 39–47
Printed in the USA.

1052-2166/04 $20.00 + .00

www.cognizantcommunication.com

Gene Expression Profiling of Fibroblasts From a Human Progeroid Disease (Mandibuloacral Dysplasia, MAD #248370) Through cDNA Microarrays

FRANCESCA AMATI,* MICHELA BIANCOLELLA,* MARIA ROSARIA D'APICE,* STEFANO GAMBARDELLA,* RUGGIERO MANGO,* PAOLO SBRACCIA,† MONICA D'ADAMO,† KATIA MARGIOTTI,* ANNAMARIA NARDONE,* MARC LEWIS,† AND GIUSEPPE NOVELLI*§

**Department of Biopathology and Diagnostic Imaging and †Department of Internal Medicine, Tor Vergata University, Via Montpellier 1, 00133 Roma, Italy*
‡Department of Psychology, The University of Texas at Austin, Austin, TX, 78703
§Division of Cardiovascular Medicine, University of Arkansas for Medical Sciences, Little Rock, AR 72205

Mandibuloacral dysplasia (MAD) is a rare autosomal recessive disorder caused basically by a missense mutation within the *LMNA* gene, which encodes for lamin A/C. We have used gene expression profiling to characterize the specificity of molecular changes induced by the prevalent MAD mutation (R527H). A total of 5531 transcripts expressed in human dermis were investigated in two MAD patients, both carrying the R527H mutation, and three control subjects (age and sex matched). Transcription profiles revealed a differential expression in MAD vs. control fibroblasts in at least 1992 genes. Sixty-seven of these genes showed a common altered pattern in both patients with a threshold expression level >±2. Nevertheless, a large number of these genes (43.3%) are ESTs or encode for protein with unknown function; the other genes are involved in biological processes or pathways such as cell adhesion, cell cycle, cellular metabolism, and transcription. Quantitative RT-PCR was applied to validate the microarray results ($R^2 = 0.76$). Analysis of the effect of the prevalent MAD mutation (R527H) over the transcriptional pattern of genes expressed in the human dermis showed that this *LMNA* gene mutation has pleiotropic effects on a limited number of genes. Further characterization of these effects might contribute to understanding the molecular pathogenesis of this disorder.

Key words: Microarray; Lamin A/C; Mandibuloacral dysplasia; QRT-PCR

MANDIBULOACRAL dysplasia (MAD; OMIM #248370) is a disorder characterized by mandibular hypoplasia, acro-osteolysis, joint contractures, poikiloderma, and lipodystrophy. We demonstrated that a homozygous missense mutation in lamin A/C (*LMNA*) is the prevalent cause of MAD (20). A recent study indicates that a subset of MAD patients carry mutations in the *ZMPSTE24* gene, an integral membrane metalloproteinase implicated in the posttranslational processing of prelamin, a precursor of lamin A (1,22). The 90 known *LMNA* mutations are responsible for 10 diseases including three muscular dystrophies (autosomal dominant and autosomal recessive Emery-Dreifuss muscular dystrophy, and limb-girdle muscular dystrophy type 1B), four segmental progerias (Hutchinson-Gilford progeria, mandibuloacral dysplasia, "atypical" Werner syndrome, cardiocutaneous progeria syndrome), a cardiac/conduction disorder (dilated cardiomyopathy with conduction defect), a neuropathy (Charcot-Marie-Tooth disorder type 2B1),

Accepted April 13, 2004.
Address correspondence to Giuseppe Novelli, Department of Biopathology and Diagnostic Imaging, Tor Vergata University, Via Montpellier 1, 00133 Roma, Italy. Tel: +39-06+20900665; Fax: +39-06-20427313; E-mail: novelli@med.uniroma2.it

and a lipodystrophy (Dunnigan-type familial partial lipodystrophy) (2,4,5,9–12,14,19,20,23). The *LMNA* gene products are nearly ubiquitously expressed, and although there is some overlap of symptoms in the diseases cited above, it is unclear how a single gene can produce such a broad spectrum of tissue-specific effects.

The molecular mechanisms by which *LMNA* mutations would cause such a broad spectrum of effects are essentially three [reviewed in (3,13,21)]: 1) an increased nuclear fragility that might be a predisposing factor to mechanical stress-induced nuclear damage and apoptosis; 2) an alteration of the bidirectional transit of large molecules, such as transcription factors, between the cytoplasm and nucleus; 3) a disruption of the chromatin organization and therefore a perturbation on gene transcription. A recent article suggests a connection between an increased nuclear fragility and gene regulation in $Lmna^{-/-}$ cells (16).

In the present study, we examined gene expression patterns in one of the laminopathies, MAD, to identify transcriptional misregulation and to improve our understanding of lamin-associated pathology. Considering that all of the cellular types affected in MAD derive from the human mesoderma, we decide to analyze the expression profile of MAD fibroblasts using a filter array, DermArray, containing over 5500 transcripts expressed in human dermis (6).

MATERIALS AND METHODS

Patient Samples

Human fibroblasts were isolated from skin biopsies (dorsal forearm) obtained from two MAD patients (20) and from three control subjects. All biopsies were obtained under institutionally approved protocols (Tor Vergata University and Italian Dermatological Institute, Rome).

MAD patients (P.W., a male, and C.E., a female) had disease onset 6 and 8 years of age, respectively, and underwent skin biopsy at 35 (P.W.) and 18 (C.E.) years of age. Both the MAD patients were homozygous for the R527H mutation and they show the same clinical phenotype without important differences (20). We collected only two patients because of the rarity of this disease (only 20 patients around the world) and the nonavailability of more Italian patients to perform a dermal biopsy. In addition, no cell lines are accessible through international cell banks.

The three control biopsies came from the IDI (Italian Dermatological Institute, Rome); one was from a 35-year-old man (control 1) and two were from a 18-year-old woman (control 2) and a 20-year-old woman (control 3). No skin pathology was reported for these individuals and for MAD patients.

RNA Purification and Labeling

Fibroblasts were grown to 80% confluence on 75-cm^2 flasks before total RNA was isolated by the TRIZOL standard protocol (Invitrogen). A small aliquot of RNA was then used for quantification and quality control using a spectrophotometer (Biophotometer, Eppendorf) and an agarose gel electrophoresis. Ten micrograms of total RNA was retro-transcribed and labeled with [^{33}P]dCTP (NEN) using a GeneFilter labeling kit (ResGen, Invitrogen, USA). Labeled cDNAs were then purified and activity was measured by a probe counter.

DermArray

DermArray (Integriderm ID1001) is a mammalian microarray containing 5531 sequence-validated human cDNA fragments on a Nylon filter membrane (6). A complete list of genes present onto the DermArray is available at the web site (www.integriderm.com). DermArray contains a system of controls, such as total genomic DNA and putative housekeeping genes. The genomic DNA spots are useful for orientation of the membrane and for grid alignment. The housekeeping genes were chosen among those that showed little expression pattern difference among different tissues. Many of the cDNAs present onto the DermArray are known genes, but ESTs of unknown function are also included. A total of 383 of the known genes are triplicated on the Nylon membrane to allow for statistical analysis of intra- and interfilter probe hybridization intensity variations or standard deviations. Each DermArray filter can be used five times after stripping; to analyze the removal of signal contaminations from the previous hybridization experiment we checked out each filter after 3-h exposition by using a phosphor imaging screen (STORM apparatus, Amersham Bioscences). Each hybridization experiment was replicated two different times for each RNA sample.

Microarray Hybridization

Microarray hybridization was carried out in roller bottles using a rotary hybridization oven (ThermoHybaid, USA) with 5 ml of a hybridization solution (MicroHyb solution, ResGen, Invitrogen). Labeled cDNAs were denatured at 95°C for 5 min and applied directly to the hybridization solution. Microarray hybridization was performed at 42°C overnight. Posthybridization washings were made according to DermArray instructions, and the removal of signals was checked out after a 3-h exposition onto a phosphor imaging screen

(STORM). Two replicates of each experiment were done using different DermArray filter derived from the same lot number.

Statistical Analysis of Expression Data

The acquisition of filter images was carried out by using a STORM apparatus (Amersham Biosciences) after a 16-h exposition. Filter images were analyzed with Pathways 4-Universal Microarray Analysis Software (ResGen). Differentially expressed genes have been identified by selecting two parameters of the Pathways software: ratio and difference. Ratio is the normalized intensity, after background correction, of one clone from the first experiment divided by normalized intensity of the same clone from the second experiment. Difference is the numerical value resulting from the subtraction of the normalized intensity of one clone on the first experiment from the normalized intensity of the same clone from the second experiment. The normalization algorithm is data point normalization, which generates normalized intensities by dividing sampled intensities by the mean sampled intensities of all clones.

Overexpressed genes are defined as those genes whose ratio is greater than 1 and the difference is a positive number; underexpressed genes are those whose ratio is less than 1 and the difference is a negative number. To increase the reliability of the results, data were managed first with a threshold greater than 2.0 and then with a threshold grater than 3.0, so that genes expressed at levels twofold or threefold greater than control levels were regarded as increased whereas genes that were expressed at levels twofold or threefold less than control levels were regarded as decreased genes. The accession number of all the genes differentially expressed found in this study was selected by using Unigene database (http://www.ncbi.nlm.nih.gov/entrez/).

To correlate expression value obtained from microarray analysis and quantitative RT-PCR we used the $\log_2$ transformation of the median value of each gene for both the patients.

Validation of Relative Gene Expression by Real-Time RT-PCR

Total RNA extracted from fibroblasts of the two patients and the three control subjects was reverse-transcribed to cDNA according to protocol of High-Capacity cDNA Archive Kit (Applied Biosystems, Foster City, CA, USA). Incubation conditions were the following: 10 min to 25°C and 2 h to 37°C. We performed real-time quantitative PCR (QRT-PCR) using the Taqman system (Applied Biosystems). The expression levels of 10 genes and an internal reference (*GAPDH*) were measured by multiplex PCR using Assay-on-Demand™ gene expression products (Applied Biosystems) labeled with 6 carboxyfluorescein (FAM) or VIC dye (Applied Biosystems). The analyzed genes were the following: Hs00157107 (*CRYAB*); Hs00268540 (*TPM2*), Hs00192399 (*PIK3CD*); Hs00426287 (*IGFBP3*); Hs00155794 (*APOD*); Hs00164103 (*COL3A1*); Hs00265358 (*POLR2B*); Hs99999903 (*ACTB*); Hs00153462 (*LMNA*); Hs00198887 (*BTG2*). The simultaneous measurement of each gene-FAM and GAPDH-VIC permitted normalization of the amount of cDNA added per sample. We performed PCRs using the Taqman Universal PCR Master Mix and the ABI PRISM 7000 Sequence Detection System. A comparative threshold cycle (C_T) was used to determine gene expression relative to a calibrator (control subjects). Hence, steady-state mRNA levels were expressed as *n*-fold difference relative to the calibrator. For each sample, our genes' C_T value was normalized using the formula $\Delta C_T = C_{tgene} - C_{tGAPDH}$. To determine relative expression levels, the following formula was used: $\Delta\Delta C_T = \Delta C_{Tsample} - \Delta C_{Tcalibrator}$ and the value used to plot relative gene expression was calculated using the expression $2^{-\Delta\Delta CT}$.

RESULTS

To establish the expression pattern of dermal fibroblasts of MAD patients we hybridized a filter array containing about 5000 genes expressed in human dermis. The expression data listed in the supplementary Table file (Dermarray MAD raw data.xls) correspond to the mean value of the two different experiments for each patient. The experiment involving patient C.E. was performed using a control RNA obtained by mixing the same quantity of total RNA from control 2 and control 3. According to the default values for ratio and difference parameters (see Materials and Methods), we selected 840 underexpressed genes and 1152 overexpressed genes. To increase the reliability of the data, we first analyzed the data considering only those genes whose differential expression had a threshold >±2.0 in both patients. A total of 67 genes resulted in differential expression in MAD fibroblasts (1.24% of the genes represented in the DermArray). Of these, 24 (36% of the differentially expressed genes) were overexpressed and 43 (64% of the differentially expressed genes) were underexpressed (Table 1). However, considering only common genes with a threshold >±3, we were able to find 11 differentially expressed genes (0.22% of the genes represented in the DermArray); of these, two genes were overexpressed and nine underexpressed (Table 1, in bold).

TABLE 1
GENES RESULTING IN DIFFERENTIAL EXPRESSION IN MAD FIBROBLASTS

Address	Gene Name	Accession No.	Patient C.E. Expression Ratio	Patient P.W. Expression Ratio	Biological Process or Molecular Function
ID1001 2670	ACTA2	AA634006	−2.5	−4.5	muscle development
ID1001 2352	ANXA1	H63077	−2.6	−3.4	signal transduction
	ANXA1	H63077	−2.2	−1.9	signal transduction
ID1001 2112	ANXA1	H63077	−2.6	−3.7	signal transduction
ID1001 2862	**APOD**	**H15842**	**3.3**	**12.6**	**lipid metabolism**
ID1001 1177	**APOD**	**AA456975**	**3.3**	**23.4**	**lipid metabolism**
ID1001 4400	APOB-100	H88540	−3.4	−2.2	lipid metabolism
ID1001 1560	ARG2	H17612	2.5	4.4	arginine catabolism
ID1001 1568	ARPC2	H25917	−2.5	−2.1	unknown
ID1001 2630	ASM3A	AA676836	−2.0	−4.3	unknown
ID1001 94	CARP	AA969184	−3.2	−2.2	unknown
ID1001 1301	CCND1	AA487486	−2.1	−11.0	regulation of cell cycle
ID1001 4879	CCNL2	AA410608	−3.5	−2.1	unknown
ID1001 3904	CD59	H60549	−2.3	−2.0	unknown
ID1001 2522	cDNA DKFZp566C0424	H94739	−2.5	−6.1	unknown
ID1001 481	CDO1	AA497033	2.2	2.6	taurine metabolism
ID1001 4224	CENTD1	AA884157	2.8	5.7	unknown
ID1001 1311	COL3A1	T98612	2.2	3.8	cell adhesion
ID1001 4112	COL3A1	T98612	2.7	5.6	cell adhesion
ID1001 1075	COL3A1	T98612	2.8	6.5	cell adhesion
ID1001 79	COX7C	AA629719	−3.0	−2.4	mitochondrial electron transport
ID1001 434	**DAPK3**	**AA973730**	**−3.6**	**−3.2**	**protein amino acid phosphorylation**
ID1001 92	DGCR5	AA970581	−3.5	−2.6	unknown
ID1001 3985	DGSI	AA463452	−8.6	−2.1	unknown
ID1001 5336	DKK3	AA425947	−4.6	−2.7	embryonic development or morphogenesis
ID1001 1225	DPT	R48303	2.8	3.3	cell adhesion
ID1001 2730	EST	AA775606	−3.0	−2.1	unknown
ID1001 2832	EST	AA707464	2.5	3.6	unknown
ID1001 1022	ESTs	AA699908	2.3	2.2	unknown
ID1001 1136	ESTs	R53431	−11.5	−2.4	unknown
ID1001 1137	ESTs	U55967	−2.3	−2.2	unknown
ID1001 1373	ESTs	AA702686	−3.1	−2.1	unknown
ID1001 1377	ESTs	AA127743	−2.5	−2.3	unknown
ID1001 1718	ESTs	AA777375	2.2	2.6	unknown
ID1001 2833	ESTs	AA707469	2.1	2.7	unknown
ID1001 3338	FEZ1	H20759	2.0	2.3	axonal outgrowth
ID1001 3664	G02S	AA931758	−2.2	−2.9	regulation of cell cycle
ID1001 3402	GAS1	AA292054	2.1	3.0	cell cycle arrest
ID1001 5062	GATM	R61229	2.3	2.1	creatine byosynthesis
ID1001 4252	GLG1	H66617	4.3	2.2	receptor binding
ID1001 2326	**GPC1**	**AA455896**	**−3.0**	**−3.2**	**unknown**
ID1001 3666	**GPS2**	**AA971634**	**−3.3**	**−4.2**	**cell cycle**
ID1001 3527	GTPBP5	AA946732	2.3	2.3	unknown
ID1001 4312	**HEMGN**	**AA431795**	**−4.5**	**−8.1**	**unknown**
ID1001 468	mRNA for KIAA0607 protein	N35489	−4.3	−2.9	unknown
ID1001 5301	HRB2	W52273	−2.2	−2.0	nucleic acid binding
ID1001 593	HREV107	AA476438	−2.0	−2.0	oncogene
ID1001 3354	HRG	H70473	2.1	3.0	unknown
ID1001 722	**IGFBP7**	**T53298**	**−6.8**	**−2.8**	**metabolism**
ID1001 962	**IGFBP7**	**T53298**	**−12.6**	**−3.6**	**metabolism**
ID1001 3761	**IGFBP7**	**T53298**	**−14.0**	**−5.7**	**metabolism**
ID1001 1037	LPP	AA047443	−3.8	−2.8	electron transport
ID1001 562	MAOA	AA011096	2.5	2.1	electron transport
ID1001 1154	**MGC16824**	**N50686**	**−8.3**	**−3.1**	**unknown**
ID1001 4343	MLCB	AA487253	−3.1	−2.8	unknown
ID1001 2296	MLH3	AA682848	−2.3	−2.3	mismatch repair

TABLE 1
CONTINUED

Address	Gene Name	Accession No.	Patient C.E. Expression Ratio	Patient P.W. Expression Ratio	Biological Process or Molecular Function
ID1001 897	OMD	N32201	2.0	2.0	cell adhesion
ID1001 769	**OSF-2**	**AA598653**	**–4.5**	**–9.8**	**cell adhesion**
ID1001 4025	PAI2	T49159	–2.9	–4.0	apoptosis
ID1001 4016	**PIP5K1B**	**R39069**	**–4.4**	**–3.9**	**phosphatidylinositol metabolism**
ID1001 1636	PLCB2	AA464970	2.5	3.1	lipid metabolism
ID1001 3925	PODXL	N64508	–2.8	–2.3	unknown
ID1001 2935	PPP1R1A	AA460827	–2.1	–2.1	glycogen metabolism
ID1001 2992	PSA	R32450	–2.1	–2.8	unknown
ID1001 4082	**RBBP1**	**AA128328**	**8.6**	**14.9**	**transcription**
ID1001 1030	**RBMS2**	**AA703090**	**–13.2**	**–5.9**	**nucleic acid binding**
ID1001 4168	RNF8	R51865	–7.3	–2.5	transcription
ID1001 1121	RPS8	AA683050	2.1	6.0	protein biosynthesis
ID1001 3957	RW1 protein	AA479691	–2.4	–3.6	unknown
ID1001 1226	SH3BP2	R48132	2.6	3.4	unknown
ID1001 688	SLC25A15	AA035452	–4.8	–2.0	amino acid metabolism
ID1001 260	**SRP68**	**AA455242**	**–3.6**	**–4.3**	**protein-ER targeting**
ID1001 3608	TCEA2	AA412500	2.1	4.0	transcription
ID1001 4704	VAV2	AA682337	5.6	2.3	signal transduction

The table lists the genes that are found over- or underexpressed in patient P.W. and patient C.E. after expression profiling experiments with a threshold >±2. Each value was obtained averaging the gene expression values found in two independent experiments. Because some genes are spotted in triplicate in the DermArray, we decided to consider their respective values independently. Signed genes with a threshold >±3 are shown in bold.

The altered expression pattern of MAD fibroblasts is summarized in Figure 1 by grouping the differentially expressed genes according to their molecular function or to the biological processes in which they are active (www.geneontology.org). The prevalent group of over- or underexpressed genes corresponds to ESTs or to poorly characterized genes that encode proteins with unknown functions (Fig. 1A, B).

In general, underexpressed genes (Fig. 1A) include those encoding for proteins involved in cellular metabolism (10%), cell cycle (7%), protein synthesis and modification (5%), nucleic acid binding (5%), and electron transport (5%), whereas overexpressed genes (Fig. 1B) comprise genes involved in lipid metabolism (8%), cell adhesion (13%), cellular metabolism (13%), and transcription regulation (8%).

To confirm DermArray results 10 genes, distributed along the entire range of variation of gene expression of MAD fibroblasts (see Supplementary Table.xls), were analyzed for differential expression by real-time quantitative PCR (QRT-PCR). Among these we selected two common overexpressed genes (*COL3A1* and *APOD*), six underexpressed genes (*CRYAB, TPM2, PIK3CD, IGFBP3, ACTB, POLR2B*), and two not differentially expressed genes (*LMNA, BTG2*). The housekeeping gene *GAPDH* was used as an internal control.

As reported in Figure 2, a Pearson correlation analysis demonstrates a statistically significant positive correlation ($R^2 = 0.76$, $p = 0.001$) between the expression values obtained with the QRT-PCR and cDNA microarray assays (see Supplementary Table.xls). Interestingly, for two overexpressed genes, *APOD* and *COL3A1*, we found a lower ratio using microarrays than using quantitative RT-PCR.

The mRNA expression values (ΔC_T) obtained by QRT-PCR of 6 of these 10 genes (*CRYAB, TPM2, APOD, COL3A1, LMNA, BTG2*) in MAD patients and controls are shown in Figure 3.

DISCUSSION

We analyzed the gene expression pattern of MAD fibroblasts of two patients carrying the prevalent LMNA mutation, R527H. Both patients present a similar clinical phenotype without significant differences (20). Our expression analysis was performed by using a cDNA filter array on which 5531 genes expressed specifically in human dermis were spotted. The individual gene expression profile of MAD fibroblasts was then compared to three unaffected controls (age and sex matched).

Sixty-seven genes with statistically significant differential expression in both patients were identified (Table 1). A great number of these transcripts are ESTs or genes whose protein products have an un-

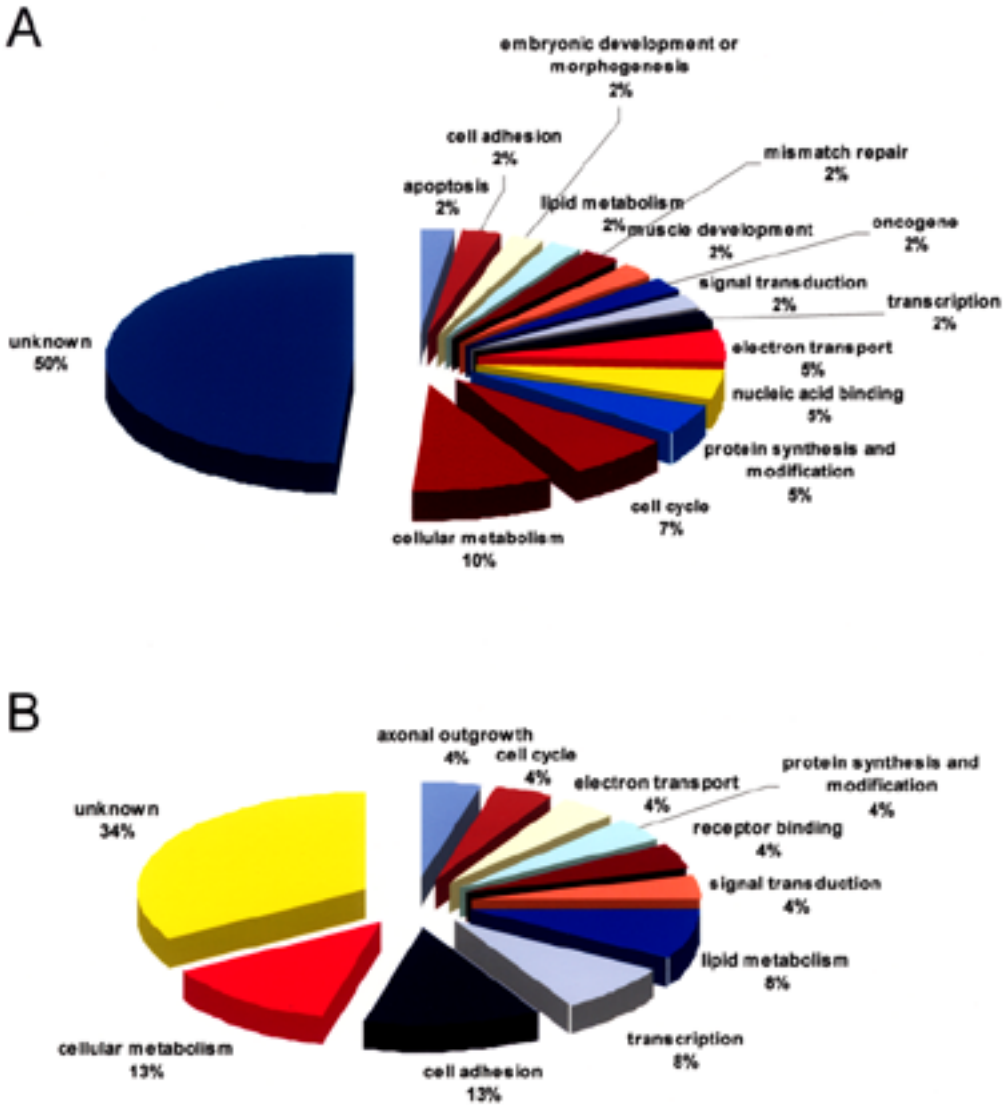

Figure 1. (A) Underexpressed genes and (B) overexpressed genes in MAD fibroblasts are grouped according to the biological process in which they are involved or to their molecular function.

known function (43.3% of the differentially expressed genes); the remaining group of altered genes contains transcripts that take part in cellular metabolism (12% of the differentially expressed genes), cell adhesion (3%), cell cycle (6%), electron transport (4.5%), lipid metabolism (4.5%), and transcription (4.5%). We speculate that some of these genes might have an important role in MAD pathogenesis and moreover they might be considered good candidate genes for the rare MAD patients without *LMNA* mutations (1). Extracellular matrix genes (e.g., dermatopontin, osteomodulin, and *COL3A1*) are overexpressed in MAD fibroblasts, reflecting maintenance of tissue integrity or regeneration (17,25,26). Genes involved in regulation and/or maintenance of cell cycle whose expression profile in MAD fibroblasts was altered are: *G0S2* (G_0/G_1 switch gene 2); *GPS2* (G protein pathway suppressor 2); *CCND1* (cyclin 1), and *GAS1* (growth arrest-specific 1). *G0S2*, which is underexpressed in MAD fibroblasts, encodes for a gene mapping on chromosome 1q32.2-q41, actively involved in the G_0/G_1 switch (24). *G0S2* expression is required to commit cells to enter the G_1 phase of the cell cycle, so the evidence that this gene is expressed at low levels (Table 1) in MAD fibroblasts might indicate a block of cell division. This is in good agreement with the overexpression of *GAS1*. In fact, *GAS1* protein is an integral plasma membrane protein whose expression is linked to growth arrest, and *GAS1* appears to be one component of a negative circuit that governs growth suppression (8). *GPS2*, which is underexpressed in MAD fibroblats, is an integral subunit of the NCOR1–

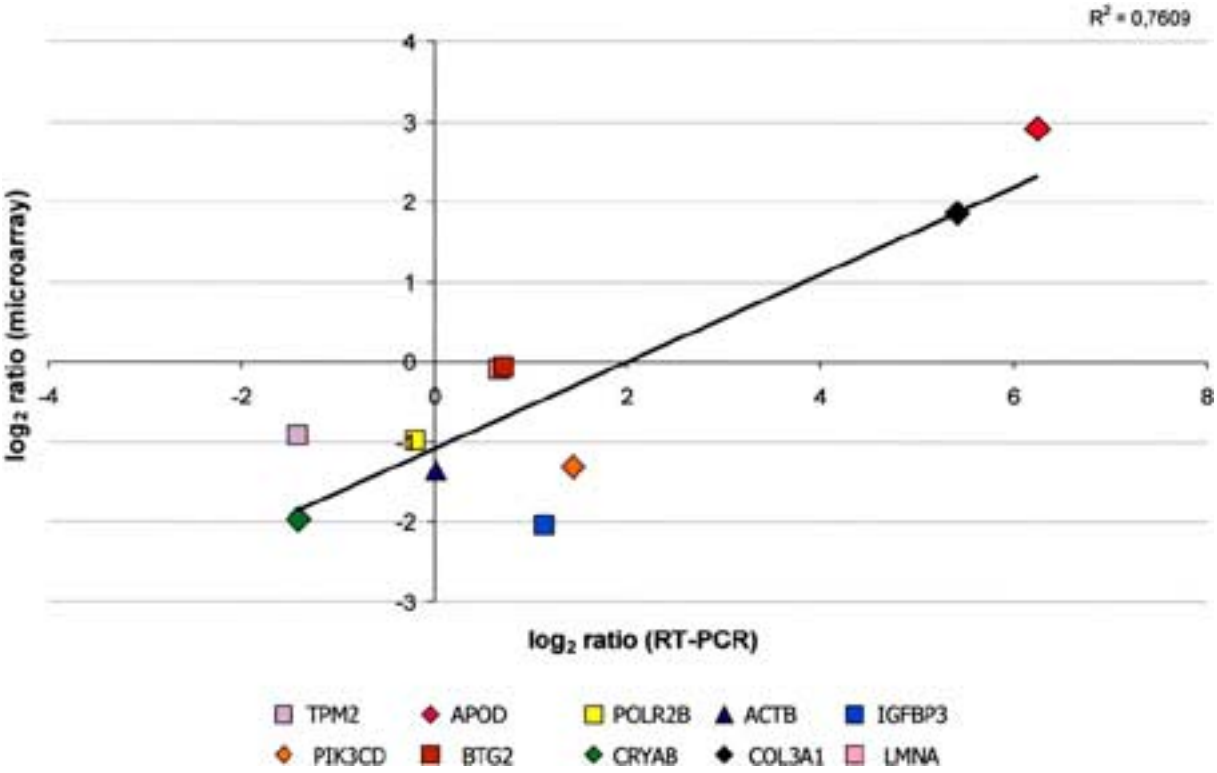

Figure 2. Comparison between data obtained from microarray and QRT-PCR experiments (expressed as $\log_2$ of the ratio values). The microarray and the QRT-PCR values for each gene are the average value of those obtained independently by the two MAD patients. The positive correlation between the two sets of data is statistically significant ($p = 0.001$).

HDAC3 complex, which is involved in the modification of chromatin structure mediated by histone deacetylases (HDACs) (28). Thus, whereas histone acetylation following recruitment of histone acetyltransferases (HATs) by promoter-bound activators facilitates transcription, histone deacetylation following recruitment of HDACs by promoter-bound repressors and co-repressors is thought to maintain a condensed chromatin state that inhibits transcription (27). In this respect, it is of interest that we have also found an increase in the mRNA levels of the *RBBP1* gene, which encodes a ubiquitously expressed nuclear pro-

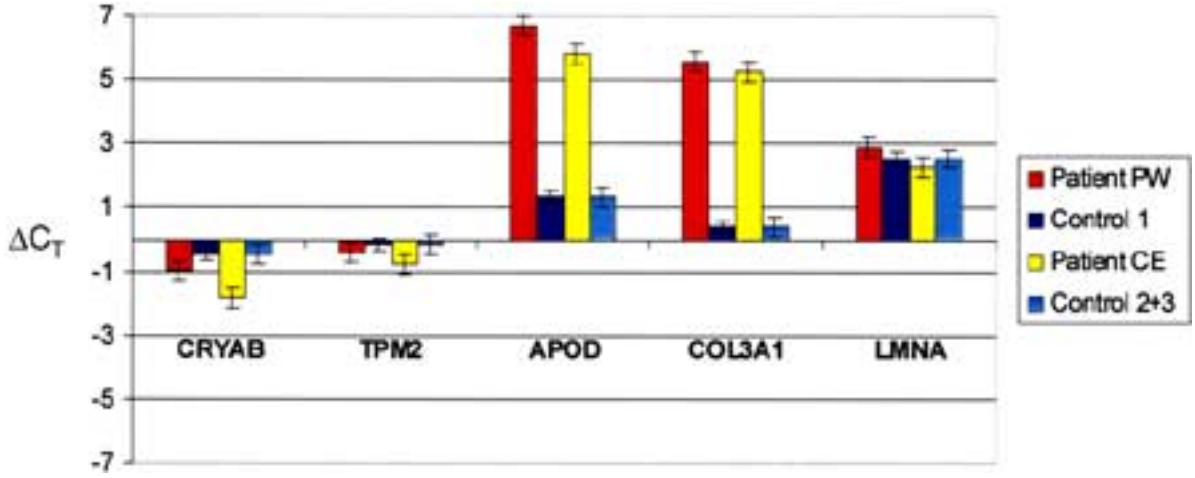

Figure 3. Histogram representing the expression levels (ΔC_T, see Materials and Methods) obtained by QRT-PCR of six differentially expressed genes in MAD patients and control subjects.

tein (7). RBBP1 protein possesses transcriptional repression activity, and it is responsible for bridging the pocket of RB family members to HDAC complexes to repress a diversity of E2F-dependent promoters (15). This is consistent with the recent observation that lamin A/C binds the active form of the retinoblastoma protein (RB), a transcriptional repressor (18). So the overexpression of a transcriptional repressor (RBBP1) in MAD fibroblasts could mean a substantial lowering of gene expression in these cell types. This result is in a good agreement with recent findings that demonstrates that *Lmna*$^{-/-}$ cells have an attenuation of transcription due to mechanical stress (16).

In this study we have applied microarray technology to identify changes in the gene expression of MAD fibroblasts. Although the study is limited to a small number of patients, this approach has allowed addressing attention to a limited number of genes, grouped in specific biological processes such as cell adhesion, cell cycle, and transcription. Nevertheless, biochemical and functional studies are necessary to confirm the biological role of these genes and their involvement in MAD pathogenesis.

ACKNOWLEDGMENTS

We would thank Aldo Mari for his technical assistance in software analysis and Paola Borgiani for statistical analysis. This work was supported by Telethon (GGP030213), the Italian Ministry of Health, and the Italian Ministry of Education, University and Research.

REFERENCES

1. Agarwal, A. K.; Fryns, J. P.; Auchus, R. J.; Garg, A. Zinc metalloproteinase, ZMPSTE24, is mutated in mandibuloacral dysplasia. Hum. Mol. Genet. 12:1995–2001; 2003.
2. Bonne, G.; Di Barletta, M. R.; Varnous, S.; Becane, H. M.; Hammouda, E. H.; Merlini, L.; Muntoni, F.; Greenberg, C. R.; Gary, F.; Urtizberea, J. A.; Duboc, D.; Fardeau, M.; Toniolo, D.; Schwartz, K. Mutations in the gene encoding lamin A/C cause autosomal dominant Emery-Dreifuss muscular dystrophy. Nat. Genet. 21:285–288; 1999.
3. Burke, B.; Stewart, C. L. Life at the edge: The nuclear envelope and human disease. Nat. Rev. Mol. Cell Biol. 3:575–585; 2002.
4. Cao, H.; Hegele, R. A. Nuclear lamin A/C R482Q mutation in Canadian kindreds with Dunnigan-type familial partial lipodystrophy. Hum. Mol. Genet. 9:109–112; 2000.
5. Chen, L.; Lee, L.; Kudlow, B. A.; Dos Santos, H. G.; Sletvold, O.; Shafeghati, Y.; Botha, E. G.; Garg, A.; Hanson, N. B.; Martin, G. M.; Mian, I. S.; Kennedy, B. K.; Oshima, J. LMNA mutations in atypical Werner's syndrome. Lancet 362:440–445; 2003.
6. Curto, E. V.; Lambert, G. W.; Davis, R. L.; Wilborn, T. W.; Dooley, T. P. Biomarkers of human skin cells identified using DermArray DNA arrays and new bioinformatics methods. Biochem. Biophys. Res. Commun. 29:1052–1064; 2002.
7. Defeo-Jones, D.; Huang, P. S.; Jones, R. E.; Haskell, K. M.; Vuocolo, G. A.; Hanobik, M. G.; Huber, H. E.; Oliff, A. Cloning of cDNAs for cellular proteins that bind to the retinoblastoma gene product. Nature 352: 251–254; 1991.
8. Del Sal, G.; Ruaro, M. E.; Philipson, L.; Schneider, C. The growth arrest-specific gene, gas1, is involved in growth suppression. Cell 70:595–607; 1992.
9. De Sandre-Giovannoli, A.; Bernard, R.; Cau, P.; Navarro, C., Amiel, J.; Boccaccia, I.; Lyonnet, S.; Stewart, C. L.; Munnich, A.; Le Merrer, M.; Levy, N. Lamin a truncation in Hutchinson-Gilford progeria. Science 300:2055; 2003.
10. De Sandre-Giovannoli, A.; Chaouch, M.; Kozlov, S.; Vallat, J. M.; Tazir, M.; Kassouri, N.; Szepetowski, P.; Hammadouche, T.; Vandenberghe, A.; Stewart, C. L.; Grid, D.; Levy, N. Homozygous defects in LMNA, encoding lamin A/C nuclear-envelope proteins, cause autosomal recessive axonal neuropathy in human (Charcot-Marie-Tooth disorder type 2) and mouse. Am. J. Hum. Genet. 70:726–736; 2002.
11. Eriksson, M.; Brown, W. T.; Gordon, L. B.; Glynn, M. W.; Singer, J.; Scott, L.; Erdos, M. R.; Robbins, C. M.; Moses, T. Y.; Berglund, P.; Dutra, A.; Pak, E.; Durkin, S.; Csoka, A. B.; Boehnke, M.; Glover, T. W.; Collins, F. S. Recurrent de novo point mutations in lamin A cause Hutchinson-Gilford progeria syndrome. Nature 423:293–298; 2003.
12. Fatkin, D.; MacRae, C.; Sasaki, T.; Wolff, M. R.; Porcu, M.; Frenneaux, M.; Atherton, J.; Vidaillet, H. J.; Spudich, S.; De Girolami, U.; Seidman, J. G.; Seidman, C.; Muntoni, F.; Muehle, G.; Johnson, W.; McDonough, B. Missense mutations in the rod domain of the lamin A/C gene as causes of dilated cardiomyopathy and conduction-system disease. N. Engl. J. Med. 341:1715–1724; 1999.
13. Hutchison, C. J. Lamins: Building blocks or regulators of gene expression? Nat. Rev. Mol. Cell. Biol. 3:848–858; 2002.
14. Judge, D. P.; Rhys, C. M. J.; Guerrerio, J.; Geubtner, J.; Zhang, J.; Cheng, A.; Dietz, H. C. 53rd Annual Meeting ASHG (P18, p. 165); 2003.
15. Lai, A.; Lee, J. M.; Yang, W-M.; DeCaprio, J. A.; Kaelin, W. G., Jr.; Seto, E.; Branton, P. E. RBP1 recruits both histone deacetylase-dependent and independent repression activities to retinoblastoma family proteins. Mol. Cell. Biol. 19:6632–6641; 1999.
16. Lammerding, J.; Schulze, P. C.; Takahashi, T.; Kozlov,

S.; Sullivan, T.; Kamm, R. D.; Stewart, C. L.; Lee, R. T. Lamin A/C deficiency causes defective nuclear mechanics and mechanotransduction. J. Clin. Invest. 113:370–378; 2004.
17. LeRoy, E. C. Increased collagen synthesis by scleroderma skin fibroblasts in vitro: A possible defect in the regulation of activation of the scleroderma fibroblast. J. Clin. Invest. 54:880–889; 1974.
18. Markiewicz, E.; Dechat, T.; Foisner, R.; Quinlan, R. A.; Hutchison, C. J. Lamin A/C binding protein LAP2 is required for nuclear anchorage of retinoblastoma protein. Mol. Biol. Cell. 13:4401–4413; 2002.
19. Muchir, A.; Bonne, G.; van der Kooi, A.J.; van Meegen, M.; Baas, F.; Bolhuis, P. A.; de Visser, M.; Schwartz, K. Identification of mutations in the gene encoding lamins A/C in autosomal dominant limb girdle muscular dystrophy with atrioventricular conduction disturbances (LGMD1B). Hum. Mol. Genet. 9: 1453–1499; 2000.
20. Novelli, G.; Muchir, A.; Sangiuolo, F.; Helbling-Leclerc, A.; D'Apice, M. R.; Massart, C.; Capon, F.; Sbraccia, P.; Federici, M.; Lauro, R.; Tudisco, C.; Pallotta, R.; Scarano, G.; Dallapiccola, B.; Merlini, L.; Bonne, B. Mandibuloacral dysplasia is caused by a mutation in LMNA-encoding lamin A/C. Am. J. Hum. Genet. 71:426–431; 2002.
21. Novelli, G.; D'Apice, M. R. The strange case of the "lumper" laminA/C gene and the human premature ageing. Trends Mol. Med. 9:370–375; 2003.
22. Pendas, A. M.; Zhou, Z.; Cadinanos, J.; Freije, J. M.; Wang, J.; Hultenby, K.; Astudillo, A.; Wernerson, A.; Rodriguez, F.; Tryggvason, K.; Lopez-Otin, C. Defective prelamin A processing and muscular and adipocyte alterations in Zmpste24 metalloproteinase-deficient mice. Nat. Genet. 31:94–99; 2002.
23. Raffaele Di Barletta, M.; Ricci, E.; Galluzzi, G.; Tonali, P.; Mora, M.; Morandi, L., Romorini, A.; Voit, T.; Orstavik, K. H.; Merlini, L.; Trevisan, C.; Biancalana, V.; Housmanowa-Petrusewicz, I.; Bione, S.; Ricotti, R.; Schwartz, K.; Bonne, G.; Toniolo, D. Different mutations in the LMNA gene cause autosomal dominant and autosomal recessive Emery-Dreifuss muscular dystrophy. Am. J. Hum. Genet. 66:1407–1412; 2000.
24. Russell, L.; Forsdyke, D. R. A human putative lymphocyte G0/G1 switch gene containing a CpG-rich island encodes a small basic protein with the potential to be phosphorylated. DNA Cell Biol. 10:581–591; 1991.
25. Shelton, D. N.; Chang, E.; Whittier, P. S.; Choi, D.; Funk, W. D. Microarray analysis of replicative senescence. Curr. Biol. 9:939–945; 1999.
26. Takeda, U.; Utani, A.; Wu, J.; Adach, E.; Koseki, H.; Taniguchi, M.; Matsumoto, T.; Ohashi, T.; Sato, M.; Shinkai, H. Targeted disruption of dermatopontin causes abnormal collagen fibrillogenesis. J. Invest. Dermatol. 119:678–683; 2002.
27. Williams, R. R. Transcription and the territory: The ins and outs of gene positioning. Trends Genet. 19: 298–302; 2003.
28. Zhang, J.; Kalkum, M.; Chait, B. T.; Roeder, R. G. The N-CoR-HDAC3 nuclear receptor corepressor complex inhibits the JNK pathway through the integral subunit GPS2. Mol. Cell 9:611–623; 2002.